

# EFFECT OF CREEP ON TIME-DEPENDENT BEHAVIOUR OF PRESTRESSED CONCRETE INTEGRAL ABUTMENT BRIDGE

**Akilu Muhammad<sup>1</sup>, Redzuan Abdullah<sup>1</sup>, Mohd Salleh Yassin<sup>1</sup>**

<sup>1</sup>*Faculty of Civil Engineering, Universiti Teknologi Malaysia, 81310 Skudai, Johor Bahru, Malaysia*

*Corresponding Author: [akilmuh@yahoo.com](mailto:akilmuh@yahoo.com)*

**Abstract:** A parametric study was conducted to assess effect of creep on long term behaviour of prestressed concrete Integral Abutment Bridge (IAB). Varying backfill soil types were provided behind the bridge abutment and the interaction was modelled using linear springs. The effect of backfill soil type on the behaviour of the bridge was assessed through 75-year time-history simulations carried out in Commercial Finite Element Software (LUSAS). CEB-FIP 1990 creep model was used to analyse the linear viscoelastic behaviour of creep. The result has shown that creep and backfill soil type have a no severe effect on the behaviour of the bridge.

*Keywords: Creep; Integral Abutment Bridge; Soil-structure interaction; Finite Element Method.*

## 1.0 Introduction

Integral Abutment Bridges (IABs) or jointless bridges are bridges constructed without conventional expansion joints and bearings, their superstructure and abutment are rigidly connected. IABs have recently become popular among Bridge Engineers due to their economic advantage; the maintenance of joints and bearings that used to be a major cost of bridge maintenance is virtually eliminated in IABs. The absence of joints adds to the redundancy of the structure thereby improving its structural performance especially during seismic loading. Despite these advantages, there are concerns that creep and temperature loading may lead to inadequate long term performances of IABs. The difficulty in predicting the behaviour of IABs is due to complex boundary condition, nonlinear behaviour associated with soil-structure interaction, temperature changes, creep and shrinkage of concrete (Kim and Laman, 2010). Paucity of design codes for IABs has resulted in numerous research works on long-term performance of IABs under temperature and time dependent loads. In many of these research works, soil-structure interaction was identified as a major factor that affects the behaviour of IABs (Huang et al. 2008, Dicleli and Erhan 2009, Kalayci et al. 2009, Noorzaei et al. 2010). It was discovered that the denser the backfill of sandy soil the more the axial forces and moments on the bridge deck (Faraji et, al 2001). Besides, Pile moments were minimized with denser backfill and lower pile restraint (Civjan and Bonczar, 2007).

Concrete Creep was discovered to have adverse effect on IABs (Kim and Laman 2010); deflection due to time dependent loading was found to be equal to the deflection from instantaneous loading (Arockiasamy and Savikumar, 2005). Pugasap et al (2009) discovered that Creep and Shrinkage led to long term top abutment displacement while bottom abutment displacement was due to time dependent effects and elastoplastic behaviour.

There is limitation of research works on the effect of creep on IABs under varying types of backfill soil. Since previous research works have established the importance soil-structure interaction on the behaviour of IABs, there is the need to understand the response of IABs to different types of backfill under creep effect. In this research a parametric study was undertaken on 75 years behaviour of long span prestressed concrete girder IAB under creep loading using finite element software, LUSAS.

## 2.0 The Bridge detail

The bridge is a 210m long concrete slab on Prestressed concrete girder IAB (Figure 1). It has seven equal Pier-to-Pier spans of 30m length (Figure 2a) and 11 equally spaced standard prestressed concrete T-beams of 2.7m depth (Figure 2c) with longitudinal length of 30m provided along the 13.9m bridge width to support 20mm thick Deck Slab. The bridge has two carriage ways of 3.65m on each of its two lanes. The girders are seated on pier caps placed transversely at 30m intervals and the pier caps are supported by three piers (Figure 1). At each end of the bridge, the longitudinal beams are embedded into 1.2m thick and 6m high abutments (Figure 2b). The abutment is supported by a pile cap sitting on 21 closely spaced 0.6 m diameter circular Piles. The whole structure acts like a single frame system with rigid connection between the superstructure and the substructure. The bridge is horizontal without skew or curvature.

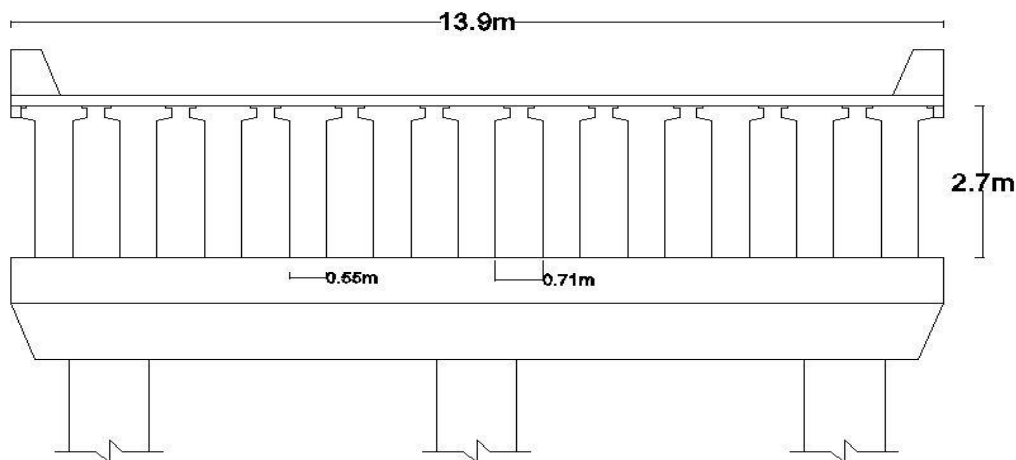
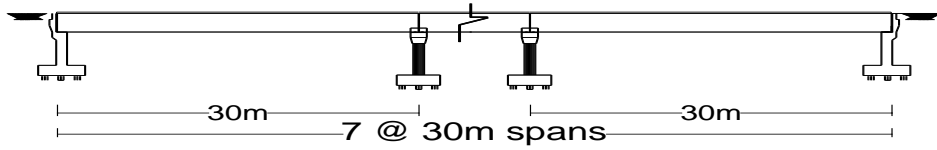
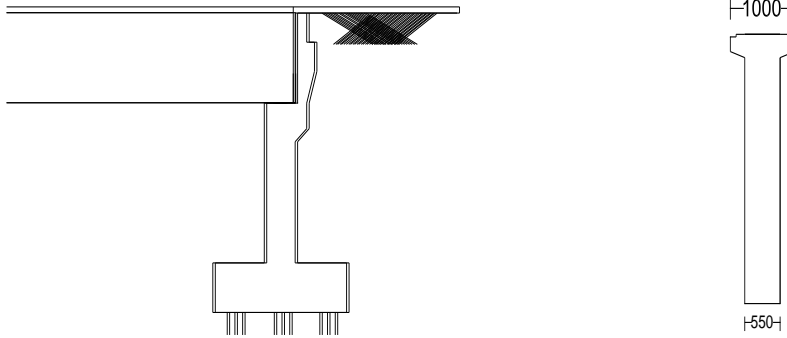


Figure 1.0: A section of the superstructure of the Integral Bridge.



(A)



(B)

(C)

Figure 2.0: (A) Elevation of the 210m long bridge. (B) Girder abutment integral connection. (C) Posttensioned T-beam (Dimensions in mm).

The bridge girders were designed as continuous Post tensioned concrete T beams. Prestress force of 4600 KN was applied on both sides of the girder using 7 wire standard strand of 12.9mm diameter and  $195E6 \text{ kN/m}^2$  Modulus of Elasticity. Secondary moments from prestress cable were analysed using equivalent load method in BPhatt (2011), and calculated using the equation:

$$q = 8x(e3 - \left(\frac{e1 + e2}{2}\right)x\left(\frac{p}{l^2}\right) \quad (1)$$

Where  $q$  is the equivalent load from cable,  $p$  is prestress force and  $x$  is the cable curvature,  $L$  is the length of a beam,  $e1$ ,  $e3$  and  $e2$  are the prestress cable eccentricities at left end, mid span and right end of the beam respectively.

### 3.0 Finite Element Model

A longitudinal strip of the bridge comprising of four beams resting on Pier cap which supported by Pier and Pile cap was used to represent the bridge model (Figure 3.0). A three-dimensional thick non-linear beam element (BTS3) with CEB-FIP1990 creep material properties, was used to model posttensioned concrete girders. Three dimensional thick beam

(BMS3) was used to model abutment wall, pier, pier head, and pile head.

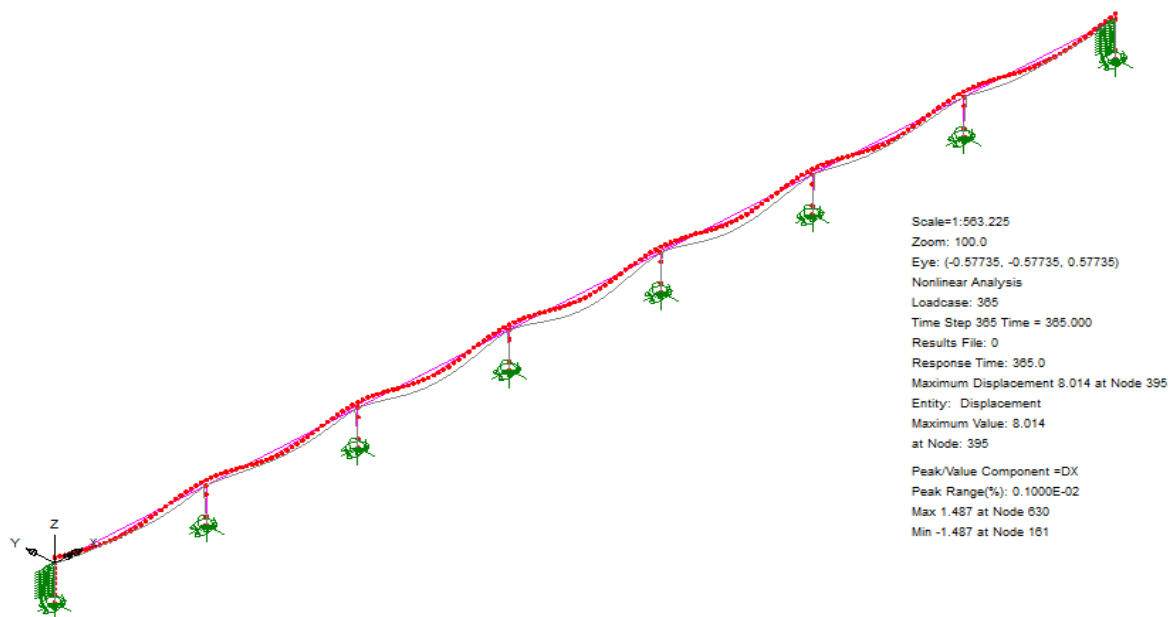


Figure 3.0 Finite Element model of the Bridge.

Tables 1 and 2 provides the geometric and materials properties of the bridge members. BS 8110 concrete grade 40 was used as the material property of all the bridge members with the exception of prestressed concrete girders which were modelled using creep material in CEB-FIP 1990 code to enable proper analysis of the effect of creep on the behaviour of the IAB.

Prestress force on girder was modelled using line mesh as shown in Figure 4.0. Horizontal line represents the beam while curved line represents tendon. Both the beam and the tendon are modelled as beam element. Single tendon prestress wizard in LUSAS calculates equivalent prestressing force from tendon and applies it to beam at nodal points. This creates the prestressing effect of tendon on the beam.



Figure 4.0 Beam and Tendon model.

The bridge loading comes from its self-weight and imposed load. Imposed load comprised of HA- UDL, HA-KEL and HA-HB 45 loads according to BD37/01 design manual of roads and bridges (British Highway Agency, 2001). Different load cases were considered for the superstructure live and dead loads and the load case that gave the worst loading condition was used in the analysis.

Table 1.0 Geometric property of Bridge members.

Member	Area (mm <sup>2</sup> )	Second moment of are about yy axis (mm <sup>4</sup> )	Second moment of are about zz axis (mm <sup>4</sup> )	Product moment of area lyz	Torsional constant Jxx
T-beam	1.81635E6	1.58525E12	54.8328E9	-93.2915E6	148.969E9
Abutment	10.2915E12	62.8587E24	1.03049E24	-4.40733E21	3.85918E24
Pier head	3.04E6	793.085E9	733.419E9	-24.0138E6	1.31989E12
Pier	6.24E6	14.0255E12	715.892E9	-0.585938	2.44947E12
Pile head	8.16E6	1.92567E12	15.6284E12	670.41E6	5.98345E12

Table 2.0 Material Properties of bridge girders.

Material	Yong Modulus Nmm	Poisson's ratio	Mass density N/mm <sup>3</sup>	Coefficient of thermal expansion	Mean compressive strength N/mm <sup>2</sup>	Relative humidity %	Nominal size mm
BS5400 Concrete creep CEB-FIP	28E3	0.2	2.4E-9	0.012E-3	50	70	462.6
BS 5400	28E3	0.2	2.4E-9	0.01E-3	50	70	462.6

#### 4.0 Creep Calculation

Concrete undergo physical and chemical change in volume as a result of its interaction with the environment. Time-dependent deformations in concrete like creep, shrinkage and relaxation are as a result of the hydration process of concrete as it interacts with the environment over time. These deformations need to be considered in studying long term behaviour of concrete. In this research, Time-history simulation was carried out to analyse the effect of creep on the long span IAB over a 75 year period in line with American State Highway and Transportation Officials (ASTHO) prescribed bridge life span period of 75 years. The nonlinear viscous behaviour of creep in concrete was analysed using CEB-FIP 1990 creep model and Modified Newton Raphson method was used for the nonlinear iteration.

CEB-FIP Model Code 1990 calculates the total strain in a concrete member that is uniaxially loaded at time  $t_0$  with a constant stress  $\sigma_c(t_0)$  as follows:

$$\varepsilon(t_0) = \varepsilon_{ci}(t_0) + \varepsilon_{cc}(t) + \varepsilon_{cs}(t) + \varepsilon_{cT}(t) \quad (2)$$

$$= \varepsilon_{c\sigma}(t) + \varepsilon_{cn}(t) \quad (3)$$

Where;

$\varepsilon_{ci}(t_0)$  is the initial strain at loading.

$\varepsilon_{cc}(t)$  is the creep strain at time  $t > t_0$

$\varepsilon_{cs}(t)$  is the shrinkage strain.

$\varepsilon_{cT}(t)$  is the thermal strain.

$\varepsilon_{c\sigma}(t)$  is the stress dependent strain:  $\varepsilon_{c\sigma}(t_0) = \varepsilon_{ci}(t_0) + \varepsilon_{cc}(t)$

$\varepsilon_{cn}(t)$  is the stress independent strain:  $\varepsilon_{cn}(t_0) = \varepsilon_{cs}(t_0) + \varepsilon_{cT}(t)$

Creep is assumed to have a linear relationship with stress within the range of service stress.

For a constant stress at time  $t_0$ , creep strain is obtained as:

$$\varepsilon_c(t) = \frac{\sigma_c(t_0)}{E_c(t_0)} [1 + \varphi(t, t_0)] \quad (4)$$

Where,  $\varphi(t, t_0)$  is creep coefficient which is a ratio of creep to instantaneous strain and  $E_c$  is Modulus of Elasticity in 28 days.

The stress dependent strain,  $\varepsilon_{c\sigma}(t, t_0)$ , may then be expressed as:

$$\varepsilon_{c\sigma}(t, t_0) = \sigma_c(t_0) \left[ \frac{1}{E_c(t_0)} + \frac{\phi(t, t_0)}{E_{ci}} \right] = \sigma_c(t_0) J(t, t_0) \quad (5)$$

Where,  $J(t, t_0)$  is the creep function,  $E_c(t_0)$  is the modulus of elasticity at the time of loading  $t_0$  and  $\frac{1}{E_c(t_0)}$  represents the initial strain per unit stress at loading.

The principle of superposition is assumed to be valid for variable stresses or strains. It is used to obtain the constitutive equation for concrete creep also known as integral type creep law as expressed in equation (6).

$$\varepsilon_c(t) = \sigma(t_0) J(t, t_0) + \int_{t_0}^t J(t, \tau) \frac{\partial \sigma_c(\tau)}{\partial \tau} \partial \tau + \varepsilon_{cn}(t) \quad (6)$$

Notional creep coefficient is estimated from the equation below:

$$\varphi(t, t_0) = \varphi_0 \beta_c(t - t_0) \quad (7)$$

$\varphi_0$  is the notional creep coefficient.

$\beta_c$  is the coefficient to describe the development of creep with time after loading.

$t$  is the age of concrete (days) at the moment considered.

$t_0$  is the age of concrete at loading (days).

In the CEB-FIP Code the notional creep coefficient is calculated from

$$\varphi_0 = \varphi_{RH} \beta(f_{cm}) \beta(t_0) \quad (8)$$

With

$$\varphi_{RH} = 1 + \frac{1 - RH / RH_0}{0.46(h/h_0)^{1/3}} \quad (9)$$

$$\beta(f_{cm}) = \frac{5.3}{(f_{cm} / f_{cm0})^{0.5}} \quad (10)$$

$$\beta(t_0) = \frac{1}{0.1 + (t_0 / t_1)^{0.2}} \quad (11)$$

Where;

$h$  is the notional size of the member (mm) =  $2Ac / u$ ,  $Ac$  is area of cross section,  $u$  is length of the perimeter of the cross section which is in contact with the atmosphere.  $f_{cm}$  is the mean concrete compressive strength (MPa) at 28 days.  $f_{cm0} = 10\text{MPa}$ ,  $RH$  is the relative humidity of the ambient environment (%),  $RH_0 = 100\%$  and  $h_0 = 100\text{mm}$  (Comite Euro-International du Beton, 1990).

The development of creep with time is given by

$$\beta_c(t - t_0) = \left[ \frac{(t - t_0) / t_1}{\beta_H + (t - t_0) / t_1} \right]^{0.3} \quad (12)$$

With

$$\beta_H = 150 \left\{ 1 + \left( 1.2 \frac{RH}{RH_0} \right)^{18} \right\} \frac{h}{h_0} + 250 \leq 1500 \quad (13)$$

## 5.0 Soil-Structure Interaction

Due to the rigid connection between the superstructure and the abutment, Backfill-Abutment interaction and Pile-Soil interaction becomes the only means of accommodation of movement from live loads, creep and shrinkage. The soil-structure interaction becomes an important factor of consideration in the behaviour of IABs. Because Piles and the Pile caps are buried in

the soil, the horizontal load on the group of Piles can be resisted by the friction and passive soil resistance (Bhatt et al, 2006). Due the rigidity provided by the supporting soil, Pile member was not considered in the model. A series of Winkler springs support is used to approximate backfill soil behavior. This is sufficient because our concern is on structural behavior of the bridge and not soil movement that may necessitate a continuum model. The horizontal spring stiffness per square meter of the backfill of stiffness  $E_s$  behind abutment of depth  $H$  and transverse length  $L$  is approximated in equation (14) ( O'Brien et al, 2005).

$$k_{horz} = \frac{(4/\pi)E_s}{(L/H)^{0.6}H} \text{ KN / m / m}^2 \quad (14)$$

$E_s$  was approximated by Lehane et al (1996) to be:

$$E_s = 150000 \frac{(2.17 - e)^2}{(1 + e)} \left( \frac{P'}{P_{atm}} \right)^{0.5} \left( \frac{0.0001}{\gamma} \right)^{0.4} \text{ KN / m}^2 \quad (15)$$

Dry density of soil  $\rho_d$ , used in specifying the degree of compaction of backfill, is related to the void ratio in equation (16) which is used in obtaining void ratio of soil.

$$\rho_d = \frac{G_s \rho_w}{(1 + e)} \quad (16)$$

Where  $G_s$  and  $\rho_w$  are the specific gravity of soil and density of water respectively,  $e$  is the void ratio of soil,  $P'$  is the mean confining stress less pore water pressure in the soil,  $P_{atm}$  the atmospheric pressure (100kN/m<sup>2</sup>),  $\gamma$  is the shear strain taken to have a range of  $50 \times 10^{-6}$  to 0.01.

Analysis of creep on the IAB was carried out under various soil types as shown in Table 3.0.

Table 3.0 Varying Soil properties used in the Model (Michael (2001) and Bowles (1996)).

Soil type	Density (wet) kN/m <sup>3</sup>	Void ratio of soil (e)	Average shear strain ( $\gamma$ ) m	Soil Stiffness kN/m <sup>2</sup>	Horizontal Spring Stiffness kN/m/m <sup>2</sup>
Dense sandy soil	22	1.0	0.0002	375771.8	6991.4
Loose sandy soil	16	1.38	0.0002	186562.6	2695.9
Medium Stiff clay	18	1.23	0.0018	31728.2	4112.1
Soft clay	15	1.47	0.0002	15788.7	2024.9



## 6.0 Result and Discussion

Finite Element Method was used to carryout 75years time history simulation to assess the effect of time-dependent loadings (creep, shrinkage and relaxation) on the behaviour of the Integral Bridge under varying backfill soil types. The result of is shown in Figures 5.0 to 12.0. The first ten years showed rapid increase in deformations (moment, shears, and deflections) where more than half of the deformations were recorded in the first ten years. This is due to the effect of shrinkage and instantaneous strains in addition to creep strain that are experienced in the early age of concrete as discussed by Raymond and Gilbert (2011). The linearity of instantaneous strain is observed in the early ages of the deformations.

Girder deflection due to time dependent loading was found to exceed girder deflection due to instantaneous loading. This is in line with findings of Arockiasamy and Savikumar, (2005) where they discovered deflection due to time dependent loading to be equal to the deflection from instantaneous loading. Figures 5 and 6 show there is no significant effect of backfill soil type on girder and abutment displacements. The maximum value of girder deflection of 9.73mm is an acceptable value within the range of safety limit. In Figure 7.0 it can be seen that there was no significant difference in the bending moment of girder due to varying backfill soil but a marked difference is observed in abutment moment. Abutment moment in soft clay soil is larger than in dense sandy soil (Figure 8.0).

Figure 9.0 shows that backfill soil type has no effect on girder axial load but there is significant difference in abutment axial load. The axial load in soft clay soil is more than thrice the value of axial load in dense sandy soil (Figure 10.0). There is also significant variation of shear in the girder and abutment under varying backfill soils over 75 years. The shear force has increased remarkably in the girder but has decreased quite significantly in the abutment (Figure 11 and 12).

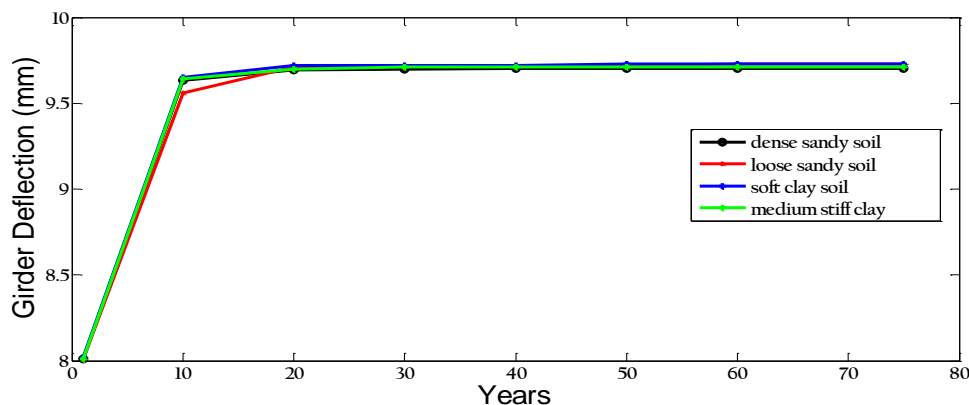


Figure 5.0 Variation of mid span Girder Displacement in 75 years under varying soil conditions.

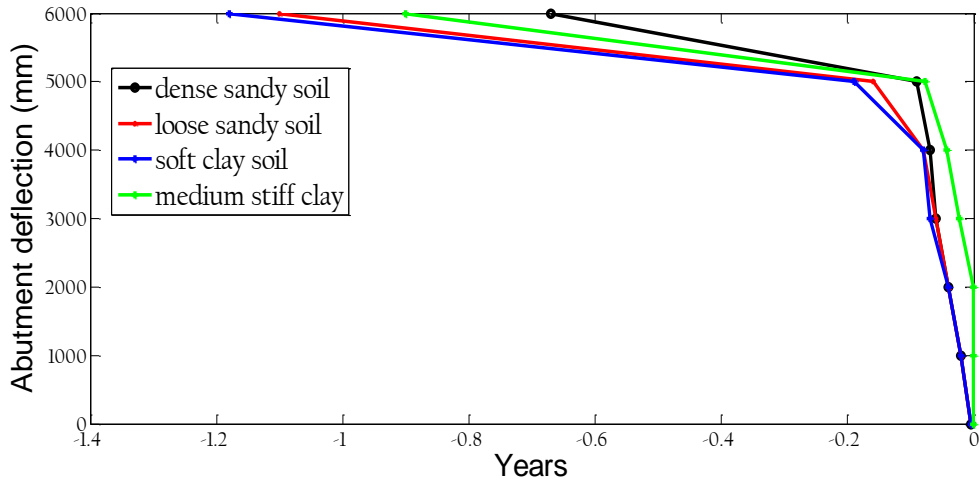


Figure 6.0 Variation of Abutment Displacement in 75 years under varying soil conditions.

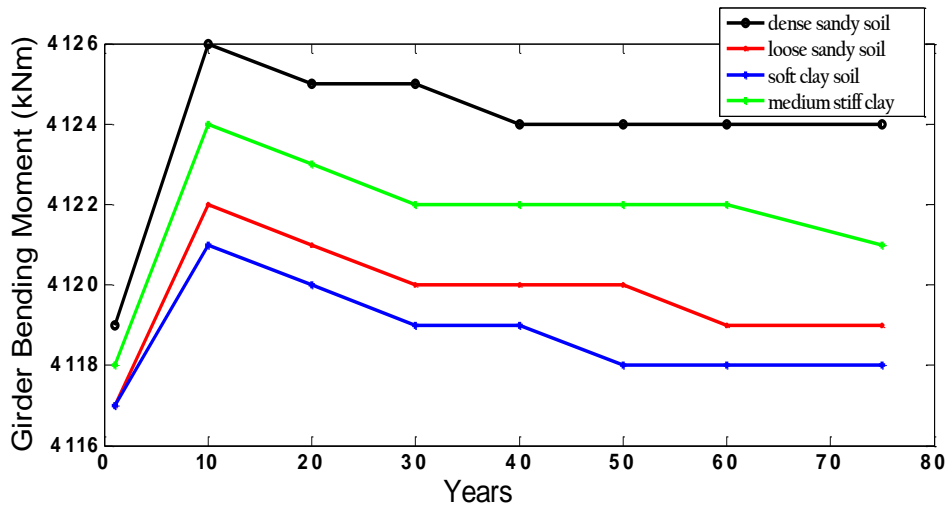


Figure 7.0 Variation Girder bending moment measures at mid span under varying soil conditions.

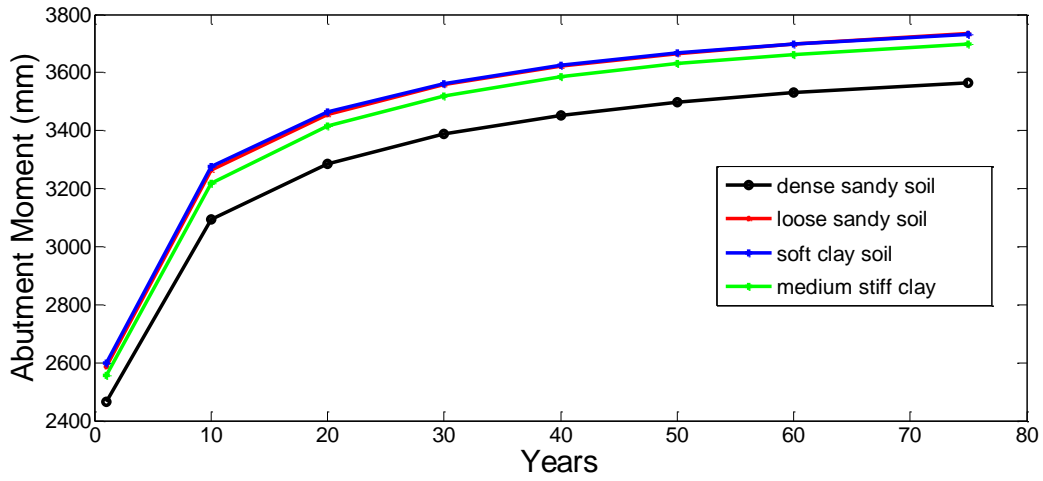


Figure 8.0 Variation of Abutment bending moment in 75years under varying soil conditions.

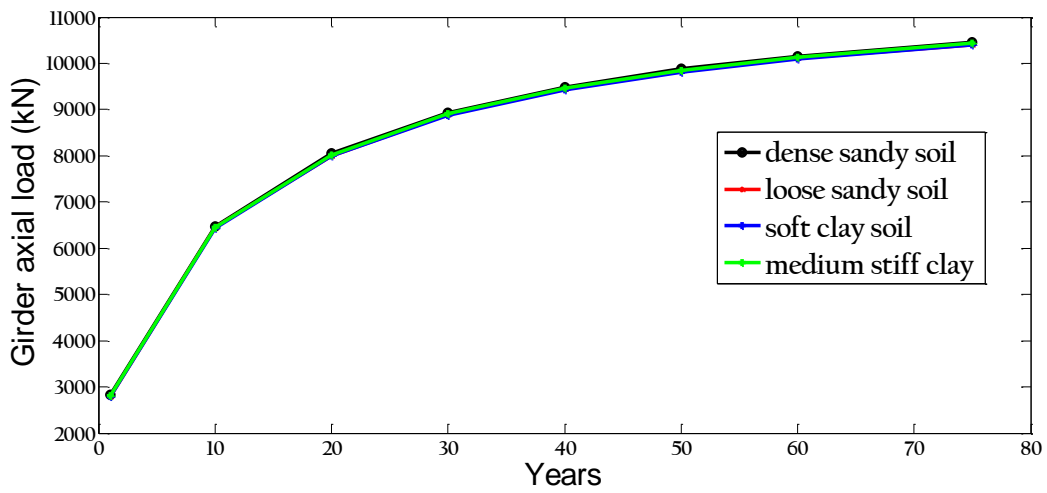


Figure 9.0 Variation of Girder axial load in 75years under varying soil conditions.

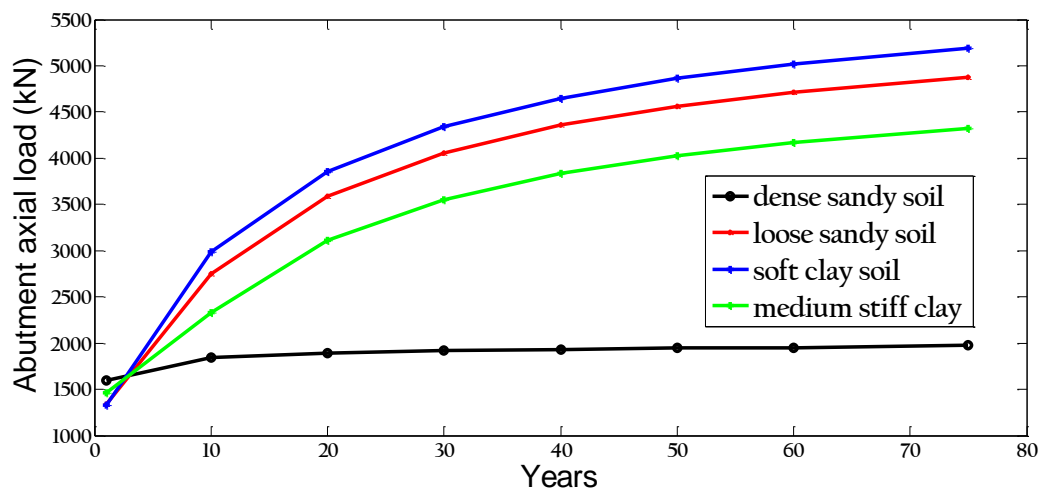


Figure 10.0 Variation of Abutment axial load in 75years under varying soil conditions.

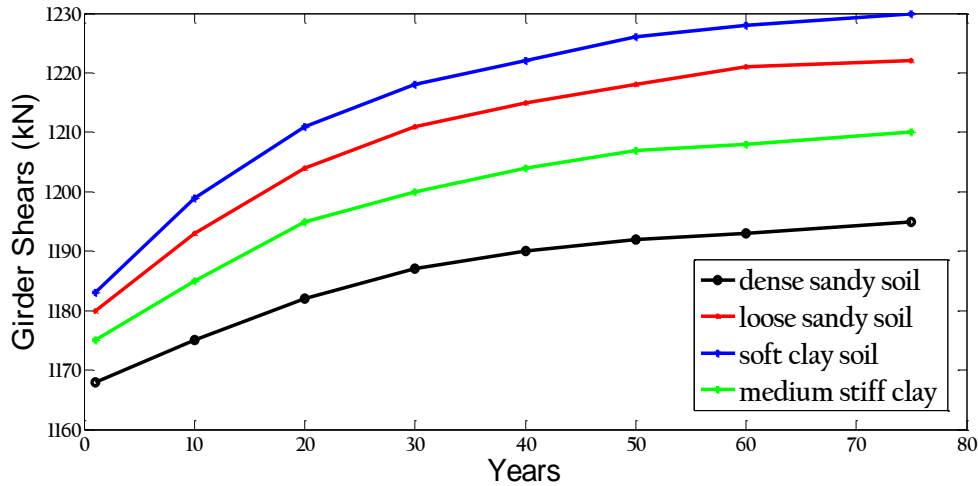


Figure 11.0 Variation of Girder Shears in 75 years under varying soil conditions.

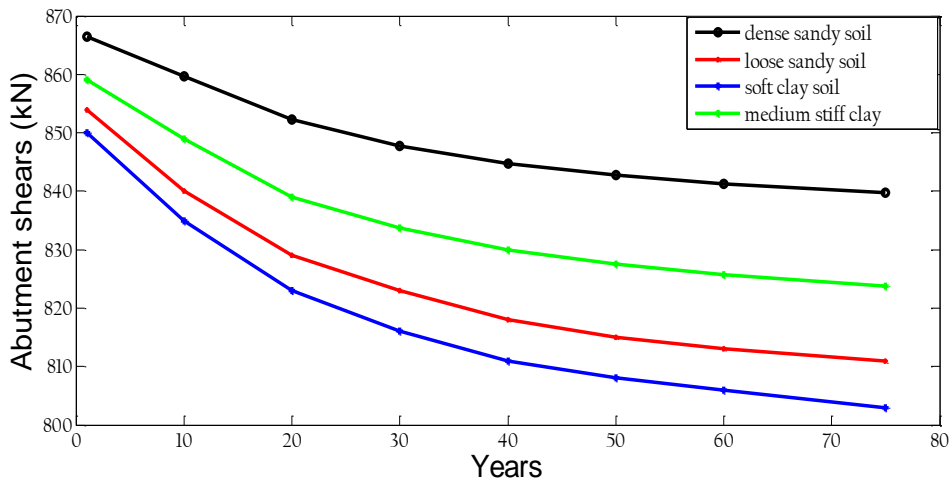


Figure 12.0. Variation of Abutment shears in 75 years under varying soil conditions.

## 7.0 Conclusion

In conclusion, the research investigated the effect of creep on long-term behaviour of Integral Abutment Bridge under varying backfill soil. The research discovered that there is no significant difference in girder and abutment displacement, girder axial load and girder moment as a result of variations in backfill soil. There is however marked variations in abutment and girder shears, abutment axial load and abutment moment.

## REFERENCES

- Arockiasamy, M., Sivakumar. M. (2005). *Time-Dependent Behaviour of Composite Integral Abutment Bridges*. Practice Periodical of Structural Design and Construction Volume 10 No.3,
- Bowles, J.E (1996) *Foundation Analysis and Design*, Fifth Edition, Mcgraw-Hill, New York,
- British Highway Authority (2001) *Design Manual for Roads and Bridges*
- Civjan, S. A., Bonczar, C., Brena, S. F., Dejong, J., & Crovo, D. (2007). *Integral abutment bridge behavior: Parametric analysis of a massachusetts bridge*. Journal of Bridge Engineering, 12(1), 64-71.
- Comite Euro-International du Beton, (1990) *CEB-FIP Model Code 1990*, Thomas Telford, Lausanne.
- Dicleli, M., & Erhan, S. (2009). *Live load distribution formulas for single-span prestressed concrete integral abutment bridge girders*. Journal of Bridge Engineering, 14(6), 472-486.
- Faraji, S., Ting, J. M., Crovo, D. S., & Ernst, H. (2001). *Nonlinear analysis of integral bridges: Finite-element model*. Journal of Geotechnical and Geoenvironmental Engineering, 127(5), 454-461.
- Huang, J., Shield, C. K., & French, C. E. W. (2008). *Parametric study of concrete integral abutment bridges*. Journal of Bridge Engineering, 13(5), 511-526.
- Kalayci, E., Breña, S. F., & Civjan, S. A. (2009). Curved integral abutment bridges - thermal response predictions through finite element analysis.
- Kim, W., & Laman, J. A. (2010). *Numerical analysis method for long-term behavior of integral abutment bridges*. [doi: 10.1016/j.engstruct.2010.03.027]. Engineering Structures, 32(8), 2247-2257.
- Lehane, B., Keogh D. L. and O'Brien E. J (1996) *Soil-Structure interaction analysis for Integral Bridges* in Advances in Computational Methods for Simulation,(ed. B.H.V. Topping), Civil-Comp Press, Edinburgh, pp.201-10.
- Michael, R. L. (2001) *Civil Engineering Reference Manual for the PE Exam*, 8<sup>th</sup> Edition, Professional Publications, Incorporated, Richmond US.
- Noorzaei, J., Abdulrazeg, A. A., Jaafar, M. S., & Kohnehpooshi, O. (2010). *Non-linear analysis of an integral bridge*. Journal of Civil Engineering and Management, 16(3), 387-394.
- O'Brien E. J., Keogh D. L., (2005). *Bridge Deck Analysis*., E & FN Spon, London.
- Prab, B. (2011) *Prestressed Concrete Design to Eurocodes*, Routledge, New York.

Prab, B., Thomas, J., Ban, S. C. (2006) *Reinforced Concrete Design Theory and Examples*, Taylor and Francis, New York.

Pugasap, K., Kim, W., & Laman, J. A. (2009). *Long-term response prediction of integral abutment bridges*. *Journal of Bridge Engineering*, 14(2), 129-139.

Raymond I. G., & Ranzi, G. (2011). *Time Dependent Behaviour of Concrete Structures* New York: Spon Press.